

# Experimental apparatus at KUR-ISOL to identify isomeric transitions from fission products, and decay spectroscopy of $^{151}\text{Ce}$

Y. Kojima <sup>a,\*</sup>, M. Shibata <sup>b</sup>, A. Taniguchi <sup>c</sup>, Y. Kawase <sup>c</sup>,  
R. Doi <sup>a</sup>, A. Nagao <sup>a</sup>, K. Shizuma <sup>a</sup>

<sup>a</sup>*Graduate School of Engineering, Hiroshima University,  
Higashi-Hiroshima 739-8527, Japan*

<sup>b</sup>*Radioisotope Research Center, Nagoya University, Nagoya 464-8602, Japan*

<sup>c</sup>*Research Reactor Institute, Kyoto University, Kumatori 590-0494, Japan*

---

## Abstract

Decay studies on  $^{151}\text{Ce}$  have been performed using the on-line isotope separator connected to the Kyoto University Reactor. In addition to conventional  $\gamma$  and conversion electron spectroscopy,  $\beta$ -gated measurements were carried out on mass-separated  $^{151}\text{Ce}$  to identify an isomeric transition. From the analysis of the obtained data, the half-life of the isotope was ascertained to be 1.76(6) s and a decay scheme containing six excited levels was constructed for the first time. The excited level at 35.1 keV in  $^{151}\text{Pr}$  was found to be a long-lived state (a half-life of approximately 10  $\mu\text{s}$  or longer).

*Key words:* radioactivity  $^{151}\text{Ce}$  [from  $^{235}\text{U}(n_{\text{th}}, f)$ ],  $\beta$ -gated measurement, long-lived level, decay scheme,  $^{151}\text{Pr}$  deduced level, mass-separation

*PACS:* 23.20.Lv, 27.70.+q

---

## 1 Introduction

Decay schemes are one of the most important information in fields of nuclear science and its applications. Many efforts, including the development of instruments and experimental techniques, have been devoted to construct decay schemes. However, our knowledge on nuclei far from stability is still left in an unsatisfied situation. The main reasons are experimental difficulties in preparing the sources and measuring them efficiently. For example, a considerable amount of data is available for the decay of Ce isotopes with a mass number  $A \leq 149$  [1]. In contrast to them, experimental data on heavier isotopes are scarce. In particular, for  $^{151}\text{Ce}$ , only a half-life value of 1.02(6) s along with energies of four  $\gamma$  rays have been reported [2]; Furthermore, no decay scheme has been proposed.

In our previous report [3], a partial decay scheme of  $^{151}\text{Ce}$  was constructed from  $\gamma$ - $\gamma$  coincidence measurements using an on-line isotope separator. However, the 35.1-keV  $\gamma$  ray, which was the most intense, could not be placed in the decay scheme because of the absence of experimentally observed cascade relationships for this transition. Subsequently, we performed additional coincidence measurements in order to obtain more comprehensive data, particularly with regard to the 35-keV  $\gamma$  ray; The detection system used in this experiment was partly reported in our previous paper [4], in which we successfully identified the  $4^-$  76.8-keV isomeric level in  $^{148}\text{Pr}$ . In this paper, we present

---

\* Corresponding author. Tel: +81-82-424-7613. Fax: +81-82-424-2453.

*Email address:* ykojima@hiroshima-u.ac.jp (Y. Kojima).

the experimental method in detail and propose the decay scheme of  $^{151}\text{Ce}$ ; It has been constructed by using data previously reported by us as well as those obtained from newly performed measurements.

## 2 Experimental methods

### 2.1 Source preparation

The  $^{151}\text{Ce}$  isotopes were prepared by the on-line isotope separator installed at the Kyoto University Reactor (KUR-ISOL) [5], following the thermal neutron-induced fission of  $^{235}\text{U}$ . A 93%-enriched  $^{235}\text{UF}_4$  target (50 mg) was irradiated with a thermal neutron flux of  $3 \times 10^{12}$  n/cm<sup>2</sup>s. The fission products thermalized in the target chamber were transported by a He-N<sub>2</sub> mixture gas jet stream to a surface-ionization-type ion source. After ionization to the chemical form of  $^{151}\text{Ce}^{16}\text{O}^+$  in order to improve the ionization efficiency, the  $^{151}\text{Ce}$  isotopes were extracted, accelerated to 30 keV and mass-separated with a resolution  $M/\Delta M$  of about 600. The mass-separated ions were implanted onto an aluminized Mylar tape in a computer-controlled tape transport system. The radioactive sources were periodically transported to a lead-shielded detector station in time intervals of 3.5 s.

### 2.2 Gamma-ray spectroscopy

Gamma-ray singles and  $\gamma$ - $\gamma$  coincidence measurements for the mass-separated  $^{151}\text{Ce}$  were performed through two experimental runs. The experimental setups for the two runs were identical except for the energy region measured. In

the first run,  $\gamma$  rays were measured in an energy range of 0–2000 keV. These experiments revealed that a spectrum in a low-energy region was complex. Therefore, in the second run, the energy region was changed to 0–1000 keV in order to obtain comprehensive data for low-energy  $\gamma$  rays. The following detectors were used in these measurements: a 30% *n*-type HPGe detector (ORTEC GAMMA-X) and a short coaxial detector (ORTEC LO-AX, crystal diameter: 51 mm, thickness: 20 mm). The energy resolution (FWHM) of the GAMMA-X was 2.2 keV at 1332 keV, and that of the LO-AX was 800 eV at 122 keV. The source-to-detector distance was 10 mm for both detectors. Energy and efficiency calibrations were performed using standard  $^{60}\text{Co}$ ,  $^{133}\text{Ba}$ ,  $^{137}\text{Cs}$  and  $^{152}\text{Eu}$   $\gamma$ -ray sources. Coincidence summing effects were considered for determining the full-energy peak efficiency. The uncertainty of the detection efficiency was estimated to be less than 10%.

In order to determine the half-life,  $\gamma$ -ray singles spectra were recorded in a multispectrum mode by using  $16 \times 4096$  channel pulse height analyzers, in which a 3.2-s counting time was divided into sixteen 0.2-s intervals. The  $\gamma$ - $\gamma$  coincidence data were recorded in an event-by-event mode. Approximately  $2.0 \times 10^6$  and  $3.2 \times 10^7$  events were accumulated during the measurement periods of 56 h and 127 h in the first and second runs, respectively.

### *2.3 Conversion electron spectroscopy*

Internal conversion electrons were measured using a 500-mm<sup>2</sup>-area and 5-mm-thick Si(Li) detector (third run). The  $^{151}\text{Ce}$  source was periodically prepared in time intervals of 3.5 s and positioned 15 mm from the Si(Li) detector surface. The energy and efficiency calibrations were performed using mass-separated

$^{146}\text{La}$ . The energy resolution of the detector was 1.7 keV for a 218-keV electron peak. In order to determine the internal conversion coefficients and obtain the cascade relations, the  $\gamma$ -ray spectra were simultaneously measured by the 30% GAMMA-X detector in singles and electron- $\gamma$  coincidence modes. The distance between the source and the HPGe detector window was 15 mm. Approximately  $5.9 \times 10^7$  events were detected over a period of 77 h. A more detailed description of this setup is provided in our previous paper [6].

#### *2.4 Beta-gated gamma and electron spectroscopy*

Electron and  $\gamma$ -ray singles,  $\beta$ -gated electron and  $\gamma$ -ray singles, and electron- $\gamma$  coincidence measurements were performed over a period of 38 h in an independent run (fourth run). The aim of this experiment was to obtain information on long-lived excited states. Details of this detection system are as follows. The Si(Li), LO-AX and a 1-mm-thick plastic scintillation detector (80 mm  $\times$  90 mm) were installed at the measuring position in a close geometry, as shown in Fig. 1. The first two of them were same to the detectors described above and the third one was used to measure  $\beta$  rays. The plastic scintillator was covered by a 0.2-mm-thick aluminum foil to absorb low-energy electrons such as internal conversion electrons. The thickness of 0.2 mm corresponds to a range for 0.2-MeV electrons. The scintillator was installed into the vacuum chamber and mounted at approximately 2 mm from the source position.

In order to evaluate the performance of this system, we introduced a  $\beta$ -gate efficiency, which was defined as the ratio between the peak count observed in the  $\beta$ -gated spectrum to that in the singles. The  $\beta$ -gate efficiency was experimentally obtained by using the transitions from mass-separated  $^{93\text{m}}\text{Y}$ ,  $^{93}\text{Sr}$

and  $^{93}\text{Rb}$ . After a measuring period of 2.6 h, the  $\beta$ -gate efficiencies were deduced for nine  $\gamma$  transitions, as shown in Fig. 2. Five transitions among them were associated to the  $\beta^-$  decay of  $^{93}\text{Rb}$ , and two among them were  $^{93}\text{Sr}$ . While maximum  $\beta^-$  ray energies to levels populating these 7 transitions varied from 2.4 to 7.2 MeV [1], the  $\beta$ -gate efficiencies were constant within their experimental uncertainties. This is due to that the energy dependence of the  $\beta$  detection efficiency is negligible in this energy region. Thus, the gate efficiency for transitions associated with  $\beta^-$  decays was deduced to be 0.278(4) as a weighted mean. A 168.5-keV  $\gamma$  ray was strongly reduced in the  $\beta$ -gated spectrum because it de-excites the isomeric state in  $^{93}\text{Y}$  ( $T_{1/2} = 0.82$  s). The  $\beta$ -gate efficiency was found to be 0.016(2) for this transition. A  $\beta$ -gate efficiency for the 590.2-keV  $\gamma$  ray showed an in-between value of 0.142(6). This is readily explained from the decay scheme shown in Fig. 2: The 590.2-keV level emitting this transition is populated by two paths, namely the  $\beta^-$  decay of  $^{93}\text{Sr}$  via high-energy states in  $^{93}\text{Y}$  and the isomeric decay of  $^{93\text{m}}\text{Y}$ . The observed gate efficiency is in good agreement with a calculated value of 0.142(7), which was deduced from averaging efficiencies for transitions due to pure  $\beta^-$  and isomeric decays weighted by their feeding intensities. Here, we note that conversion electrons from the isomeric state were not detected by the scintillator because they were completely absorbed by the aluminum foil. For the  $\beta$ -electron coincidence system, the gate efficiencies were obtained in the same way: 0.271(27) for the 214-keV K electrons from  $^{93}\text{Rb}$ , and 0.0230(35) for the 169-keV K electrons from  $^{93\text{m}}\text{Y}$ . They agree with the values for the  $\gamma$  detection system well. From what has been described above, we concluded that this detection system was sufficiently capable of determining whether a  $\gamma$  transition of interest is associated with a long-lived isomeric state. Here, “long life” implies half-life  $T_{1/2} \gtrsim 10 \mu\text{s}$  because the time range of the time-to-amplitude

converters employed was set to  $2 \mu\text{s}$  and the gate period of our coincidence system was  $5 \mu\text{s}$ .

### 3 Results

#### 3.1 Gamma ray

For the mass fraction  $A = 151 + 16$ , some  $\gamma$  rays with a half-life of approximately 2 s were newly observed together with those from  $^{151}\text{Pr}$  ( $T_{1/2} = 18.90 \text{ s}$ ) and  $^{151}\text{Nd}$  ( $T_{1/2} = 12.44 \text{ min}$ ). Figure 3 shows a  $\gamma$ -ray spectrum measured with the short coaxial HPGe detector in the second run. The half-life for each  $\gamma$  ray was determined by the least square fitting method using a single-component exponential function (Table 1 and Fig. 4). Next, 1.76(6) s was estimated as a weighted mean. The half-life of Pr KX rays could not be ascertained because their intensity was very weak and their peak overlapped with strong 35.1-keV  $\gamma$  and Nd KX rays. Table 1 summarizes  $\gamma$  rays that decay with a half-life of  $\sim 1.76 \text{ s}$ . The highest energy of the new short-lived  $\gamma$  rays was 636.8 keV while the  $\gamma$  rays were measured in the energy range of 0–2000 keV. These new  $\gamma$  rays are candidates for those from the  $\beta^-$  decay of  $^{151}\text{Ce}$ . This is because their half-life of  $\sim 2 \text{ s}$  is considerably shorter than that of other neutron-rich isobars with  $A = 151$  and no contaminations due to the neighboring masses were observed. In order to explicitly confirm the origin,  $\gamma$ -X and  $\gamma$ - $\gamma$  coincidence relations were investigated using the list data obtained in the first and second runs. As shown in Table 1, most of the  $\gamma$  rays were coincident with the Pr KX rays. In addition, from the analysis of the data from the fourth run, we found that all  $\gamma$  rays except for the 35.1-keV one were coincident with  $\beta$

rays; The details will be described in section 3.3. The 363.7- and 597.9-keV  $\gamma$  rays were not coincident with any X rays. However, they were in cascade with the 39-keV line, which was coincident with the Pr KX rays. Also, no coincidence relations were observed for the 35.1- and 636.8-keV  $\gamma$  rays. These  $\gamma$  rays, however, decayed with a half-life of  $\sim 1.8$  s and 1.71(13) s, respectively. They were consistent with the half-life value of 1.77(7) s deduced from other peaks. Therefore, we concluded that the eleven  $\gamma$  rays shown in Table 1 were associated with the  $\beta^-$  decay of  $^{151}\text{Ce}$ .

The  $\gamma$ -ray intensities relative to the 636.8-keV peak were mainly obtained using the singles data. The 35.1-, 38.9-, and 597.9-keV  $\gamma$  rays were doublets with a  $\gamma$  or X ray. Thus, their intensities were evaluated by the following analysis.

The 35.1-keV peak was a doublet of  $^{151}\text{Ce}$  and  $^{151}\text{Pr}$   $\gamma$  rays. The  $\gamma$  intensity associated with  $^{151}\text{Ce}$  was estimated by two independent methods. First, the 35.1-keV Ce peak count was obtained after subtracting the contribution from the 35.2-keV Pr  $\gamma$  ray. The 35.2-keV Pr peak count was evaluated from the experimental 22.5-keV Pr  $\gamma$ -ray counts and from their intensities reported by Shibata et al.[7]:  $I_\gamma=12.8(13)$  for the 35.2-keV and  $I_\gamma=8.3(6)$  for the 22.5-keV Pr  $\gamma$  ray. The intensity ratio of the 35.1-keV Ce to the doublet counts,  $R = I(\text{Ce})/(I(\text{Ce}) + I(\text{Pr}))$ , was found to be 48(14)%. Second, the Ce  $\gamma$ -ray count was evaluated by analyzing the decay curve of the 35-keV multiplet. The time-dependent peak counts were fitted by a three-component function: two of the functions are exponential and correspond to the decay of Ce and Pr, and third one corresponds to the growth-and-decay component of the Pr  $\gamma$  ray. In this analysis, the half-life values for Ce and Pr were fixed at 1.76 s and 18.9 s, respectively. From the least square fitting, the intensity ratio  $R$

was found to be 43(2)%, which is consistent with the value obtained by the first method. Therefore, the 35.1-keV Ce peak intensity relative to that of the 636.8-keV  $\gamma$  ray was evaluated to be 450(73) by averaging the values obtained by the two methods. At this point, it should be noted that an additional analysis was performed to confirm the validity of our assumption that the half-life of the 35.1-keV Ce peak is 1.76 s. In order to verify this assumption, a decay curve containing only the 35.1-keV Ce  $\gamma$  ray was constructed after subtracting the 35.2-keV Pr  $\gamma$ -ray counts. Here, the Pr contributions were evaluated using the 22.5-keV  $\gamma$ -ray counts, as described above. The decay curve was well represented by a single-component exponential function (Fig. 4(b)), after which a half-life value of 1.79(25) s was obtained. Therefore, we concluded that the 35.1-keV Ce peak decayed with the adopted half-life value of 1.76 s. In other words, the excited state emitting the 35.1-keV  $\gamma$  ray has a considerably shorter half-life than that of  $^{151}\text{Ce}$  (1.76 s). The discussion to be given in section 3.3 will refer to these results.

The 38.9-keV  $\gamma$  ray is a doublet with the Pm  $K_{\alpha}$ X ray. The  $K_{\alpha}$ X-ray count was evaluated from the experimentally observed Pm  $K_{\beta_2}$ X-ray count, the intensity ratio  $K_{\alpha}/K_{\beta_2}$  of 24.4(6) [1], and their detection efficiencies. After subtracting the X-ray count, the relative intensity of the 38.9-keV  $\gamma$  ray was evaluated to be 146(35).

The 597.9-keV Ce  $\gamma$  ray is a doublet with the 599.1-keV Pr  $\gamma$  transition. Because the 598-keV Ce  $\gamma$  ray was coincident with the 39-keV  $\gamma$  ray, the relative intensity of 17.2(44) was readily obtained from the spectrum gated by the 39-keV  $\gamma$  ray. In addition, the intensity was also estimated by analyzing a decay curve of this doublet. From this analysis, the intensity was found to be 14.8(46). This was consistent with the value evaluated from the coincidence

data. The averaged intensity of 16.1(32) was adopted for the 598-keV  $\gamma$  ray.

### 3.2 *Internal conversion electron*

A conversion electron spectrum was obtained in an energy range of  $\sim 30$  keV to 1000 keV. Twenty transitions from the  $\beta^-$  decay of  $^{151}\text{Pr}$  were clearly observed, and their internal conversion coefficients were deduced as reported in our previous paper [6]. However, the electron peaks associated with the  $\beta^-$  decay of  $^{151}\text{Ce}$  were not observed in this spectrum. This implies that  $\gamma$  transitions from  $^{151}\text{Ce}$  have low multiplicities.

### 3.3 *Long-lived excited state in $^{151}\text{Pr}$*

The  $\beta$ -gate efficiency, which is the ratio of counts observed in the  $\beta$ -gated spectrum to those observed in the singles, was deduced for each peak. The  $\beta$ -gate efficiencies for most of the peaks were approximately 0.3, which was consistent with the value obtained from the calibration measurements using the  $\beta$ -decay isotopes of  $^{93}\text{Sr}$  and  $^{93}\text{Rb}$ . This implies that these transitions occur due to  $\beta^-$  decays and that the excited states emitting them have very short life-time values.

A small  $\beta$ -gate efficiency was observed only for the 35-keV  $\gamma$  ray. The inset of Fig. 3 shows that the 35-keV peak in the  $\beta$ -gated spectrum has significantly reduced in comparison to that of the Nd  $\text{K}_{\beta}\text{X}$  ray. It should be noted that the 35-keV peak is a doublet of the  $^{151}\text{Ce}$  35.1-keV and the  $^{151}\text{Pr}$  35.2-keV  $\gamma$  rays. After subtracting the contribution of  $^{151}\text{Pr}$ , which was evaluated by analyzing the decay curve, the  $\beta$ -gate efficiency of the  $^{151}\text{Ce}$  35.1-keV  $\gamma$  ray

was ascertained as 0.021(3). This value agrees with the  $\beta$ -gate efficiency of 0.016(2), which was obtained for the isomeric transition from  $^{93\text{m}}\text{Y}$  in the calibration measurement. Therefore, we conclude that a level de-excited by the 35.1-keV  $\gamma$  ray has a long life. Unfortunately, the half-life of this level could not be determined exactly in this study; No sloop due to the 35.1-keV  $\gamma$  transition was observed in the time spectrum of the coincidence events. The only manner in which the half-life can be described is that it is longer than  $\sim 10 \mu\text{s}$  but considerably shorter than the  $\beta^-$ -decay half-life of  $^{151}\text{Ce}$  (1.76 s). This is because the 35.1-keV  $\gamma$  ray decays with  $T_{1/2} \sim 1.76 \text{ s}$ , as described in section 3.1; In other words, the 35-keV  $\gamma$  transition and the  $\beta^-$  decay of  $^{151}\text{Ce}$  are in radioactive equilibrium.

### 3.4 Decay scheme

A new decay scheme of  $^{151}\text{Ce}$  was constructed on the basis of  $\gamma$ -ray energies, intensities, half-lives and coincidence relationships (Fig. 5). All the levels except for the 35.1-keV level were supported by  $\gamma$ - $\gamma$  coincidence relations. The 35-keV  $\gamma$ -ray was placed as a transition from a long-lived 35-keV level to the ground state because it was not coincident with any  $\beta$  rays,  $\gamma$  rays and conversion electrons. The energy of the 362.1-keV  $\gamma$  ray was very similar to that of the 362.0-keV level, which was established from 38.9-323.1 and 323.1-40.6 keV  $\gamma$  cascades. Thus, the 362-keV  $\gamma$  ray was placed between the 362-keV and the ground level while no coincidence relation between the 41- and 362-keV  $\gamma$  rays was observed.

## 4 Discussion

### 4.1 Comparison with previous studies

The 84.8- and 118.6-keV  $\gamma$  rays with a half-life of 1.02(6) s have been assigned to the  $\beta^-$  decay of  $^{151}\text{Ce}$  in Nuclear Data Sheets [2]. They were identified from X- $\gamma$  coincidence measurements for fission products of the spontaneous fission of  $^{252}\text{Cf}$ . The 52.6- and 96.8-keV  $\gamma$  rays were also found from X- $\gamma$  coincidences for fission fragments of  $^{252}\text{Cf}$  and assigned as transitions from the  $\beta^-$  decay of  $^{151}\text{Ce}$  [2]. However, these four  $\gamma$  rays were not observed in our studies. Although experimental methods in previous studies were able to determine the atomic number, the identification of the mass number remains ambiguous. This contrasts strikingly with our experiments using the on-line mass separator. Therefore, a possible explanation for this discrepancy is the assignment of incorrect mass number in the previous studies. Another interpretation is that an unknown isomeric state exists in  $^{151}\text{Ce}$  and that the  $\beta^-$ -decay of this isomer feeds bands different from those observed in our experiments using the  $^{235}\text{U}(n_{\text{th}}, f)$  reaction. Recent studies [8] appear to partially favor this argument; These studies investigated the fission products of  $^{252}\text{Cf}$  by using the Gammasphere array and observed a 96.0-keV transition in a  $^{151}\text{Pr}$   $\gamma$  sequence.

### 4.2 Log-ft values

From the systematics of  $N = 93$  isotones, the  $3/2^-$  [521] and  $5/2^+$  [642] Nilsson orbits are possible candidates for the ground state of  $^{151}\text{Ce}$ . Hoellinger et al. [9] proposed the spin and the parity  $I^\pi$  of  $5/2^+$  for the ground state on the

basis of a level spacing of the rotational band observed in  $^{151}\text{Ce}$ . For  $^{151}\text{Pr}$ ,  $I^\pi = (3/2)^-$  was assigned to the ground state from the experimental  $\log ft$  values [7]. Thus, a  $\beta^-$  decay from  $^{151}\text{Ce}$  to the ground state of  $^{151}\text{Pr}$  is the first forbidden non-unique transition. This implies that a  $\log ft$  value for this  $\beta$  feeding is greater than 5.9 [10], i.e., the  $\beta$  transition probability is less than 7%. Here, we used the  $\log f$  table [11] and a  $Q_\beta$  value of 5.27 MeV, which was measured with a total absorption BGO spectrometer [12]. Subsequently, the  $\log ft$  values for excited levels in  $^{151}\text{Pr}$  were evaluated using the  $\beta$  feeding intensities estimated from the  $\gamma$  intensity imbalance for each level. It should be noted here that  $\beta$  transition intensities are not determined explicitly. This is because multiplicities of  $\gamma$  rays, that is, the total intensities of the  $\gamma$  rays are unknown. Thus, in this evaluation, various multiplicities,  $1 \leq l \leq 2$ , were assumed for  $\gamma$  rays in order to estimate the internal conversion coefficients [13], i.e., the total  $\gamma$  transition probabilities. As expected, the  $\log ft$  values considerably vary with the assumed multiplicities. The  $\log ft$  value for the 35-keV level, however, was approximately 4.8 for all calculation sets because the 35.1-keV  $\gamma$  intensity is considerably larger than that of the others. This small  $\log ft$  value implies that the  $\beta$  feeding to the 35-keV level is an allowed transition. Then, the  $I^\pi$  of  $(3/2^+, 5/2^+, 7/2^+)$  was assigned to the 35-keV level. When the 35-keV level is a  $3/2^+$ ,  $5/2^+$ , or  $7/2^+$  state, the  $\gamma$  transition to the  $(3/2)^-$  ground state would be E1, E1, or M2, respectively. According to the Weisskopf estimate [14], the total half-life of a 35-keV E1 transition is 3 ps and that of M2 is 80  $\mu\text{s}$  although the E1 and M2 transitions are frequently hindered by orders of  $\sim 5$  and  $\sim 1$ , respectively. The experimental results that indicated that the 35-keV level has a long life appear to favor the  $I^\pi$  of  $(7/2^+)$  for this level.

## 5 Conclusions

We have shown that the  $\beta$ -gated detection system installed to the KUR-ISOL had a sufficient ability to identify isomeric transitions. Using this apparatus and conventional  $\gamma$  and conversion electron detectors, a decay study on  $^{151}\text{Ce}$  was performed; A decay scheme of  $^{151}\text{Ce}$  was newly proposed, and a long-lived ( $\gtrsim 10\mu\text{s}$ ) excited level in  $^{151}\text{Pr}$  was identified at 35.1 keV. From the  $\log ft$  value and empirical rules, the spin and parity of  $(7/2^+)$  were tentatively assigned to this level.

## Acknowledgment

We would like to thank Dr. E. Yoshida, Mr. T. Hanafusa, Mr. O. Suematsu, and Ms. M. Hirano for their assistance in the early stages of this study. This study was performed under the Research Collaboration Program of Research Reactor Institute, Kyoto University. This work was partly supported by Grants-in-Aid for Scientific Research (No. 12780386) from the Ministry of Education, Science, Sports and Culture, Japan.

## References

- [1] R.B. Firestone and V.S. Shirley (Ed.), Table of Isotopes, John Wiley & Sons, New York, 1996.
- [2] B. Singh, Nucl. Data Sheets 80 (1997) 263.
- [3] Y. Kojima, M. Shibata, A. Taniguchi, Y. Kawase, T. Hanafusa, E. Yoshida,

- K. Shizuma, Proc. Int. Conf. on Nuclear Data for Science and Technology, Tsukuba, 2001, pp.489-492.
- [4] Y. Kojima, A. Taniguchi, M. Shibata, E. Oyama, T. Nishimura, K. Shizuma, Y. Kawase, Eur. Phys. J. A 19 (2004) 77.
- [5] A. Taniguchi, K. Okano, T. Sharshar, Y. Kawase, Nucl. Instr. and Meth. A 351 (1994) 378.
- [6] Y. Kojima, M. Shibata, A. Taniguchi, T. Hanafusa, E. Yoshida, K. Shizuma, Y. Kawase and S. Yamada, Eur. Phys. J. A 16 (2003) 331.
- [7] M. Shibata, T. Ikuta, A. Taniguchi, A. Osa, A. Tanaka, H. Yamamoto, K. Kawade, J.-Z. Ruan, Y. Kawase and K. Okano, J. Phys. Soc. Jpn. 63 (1994) 3263.
- [8] J.K. Hwang, A.V. Ramayya, J.H. Hamilton, E.F. Jones, P.M. Gore, S.J. Zhu, C.J. Beyer, J. Kormicki, X.Q. Zhang, L.K. Peker, B.R.S. Babu, T.N. Ginter, G.M. Ter-Akopian, Yu.Ts. Oganessian, A.V. Daniel, W.C. Ma, P.G. Varmette, J.O. Rasmussen, I.Y. Lee, J.D. Cole, R. Aryaeinejad, M.W. Drigert, M.A. Stoyer, S.G. Prussin, R. Donangelo and H.C. Griffin, Phys. Rev. C 62 (2000) 044303.
- [9] F. Hoellinger, N. Schulz, J.L. Durell, I. Ahmad, M. Bentaleb, M.A. Jones, M. Leddy, E. Lubkiewicz, L.R. Morss, W.R. Phillips, A.G. Smith, W. Urban and B.J. Varley, Phys. Rev. C 56 (1997) 1296.
- [10] S. Raman and N.B. Gove, Phys. Rev. 7 (1973) 1995.
- [11] N.B. Gove and M.J. Martin, Nucl. Data Tables 10 (1971) 205.
- [12] M. Shibata, Y. Kojima, H. Uno, K. Kawade, A. Taniguchi, Y. Kawase, S. Ichikawa, F. Maekawa and Y. Ikeda, Nucl. Instr. and Meth. A 459 (2001) 581.

- [13] F. Rösler, H.M. Fries, K. Alder, and H.C. Pauli, *Atom. Data and Nucl. Data Tables* 21 (1978) 91.
- [14] J.M. Blatt and V.F. Weisskopf, *Theoretical Nuclear Physics*, John Wiley & Sons, New York, 1952.

Table 1

Gamma- and X-rays assigned to the  $\beta^-$  decay of  $^{151}\text{Ce}$  and their coincidence relations. A half-life value for each  $\gamma$  ray observed in singles measurements is also presented; A weighted mean of 1.76(6) s was determined from them.

Energy (keV)	Relative Intensity	Coincident $\gamma$ /X rays (keV)	Half-life (s)
Pr KX	—	(Pr KX) <sup>1)</sup> , 39, 41, 142, (323) <sup>1)</sup>	—
35.1(1)	450(73) <sup>2)</sup>	—	(1.79(25)) <sup>2)</sup>
38.9(1)	146(35) <sup>2)</sup>	Pr KX, 41, 323, 364, 429, 598	(2.4(10)) <sup>2)</sup>
40.6(3)	22.4(20)	Pr KX, 39, 323	1.75(16)
142.1(1) <sup>3)</sup>	9.9(10)	Pr KX	1.74(26)
323.1(1)	45.4(41)	Pr KX, 39, 41	1.71(18)
362.1(1)	70.8(62)	(Pr KX) <sup>1)</sup>	1.79(8)
363.7(2)	11.9(18)	39	1.60(47)
402.5(4)	37.4(42)	(Pr KX) <sup>1)</sup>	2.4(8)
428.8(2)	6.8(19)	(Pr KX) <sup>1)</sup> , 39	1.7(5)
597.9(3)	16.1(32) <sup>2)</sup>	39	( $\sim 1.8$ ) <sup>2)</sup>
636.8(2)	100(7)	—	1.71(13)

<sup>1)</sup> Observed very weakly in the gated spectrum.

<sup>2)</sup> Estimated after subtracting contaminations (see text).

<sup>3)</sup> Not placed in the decay scheme.

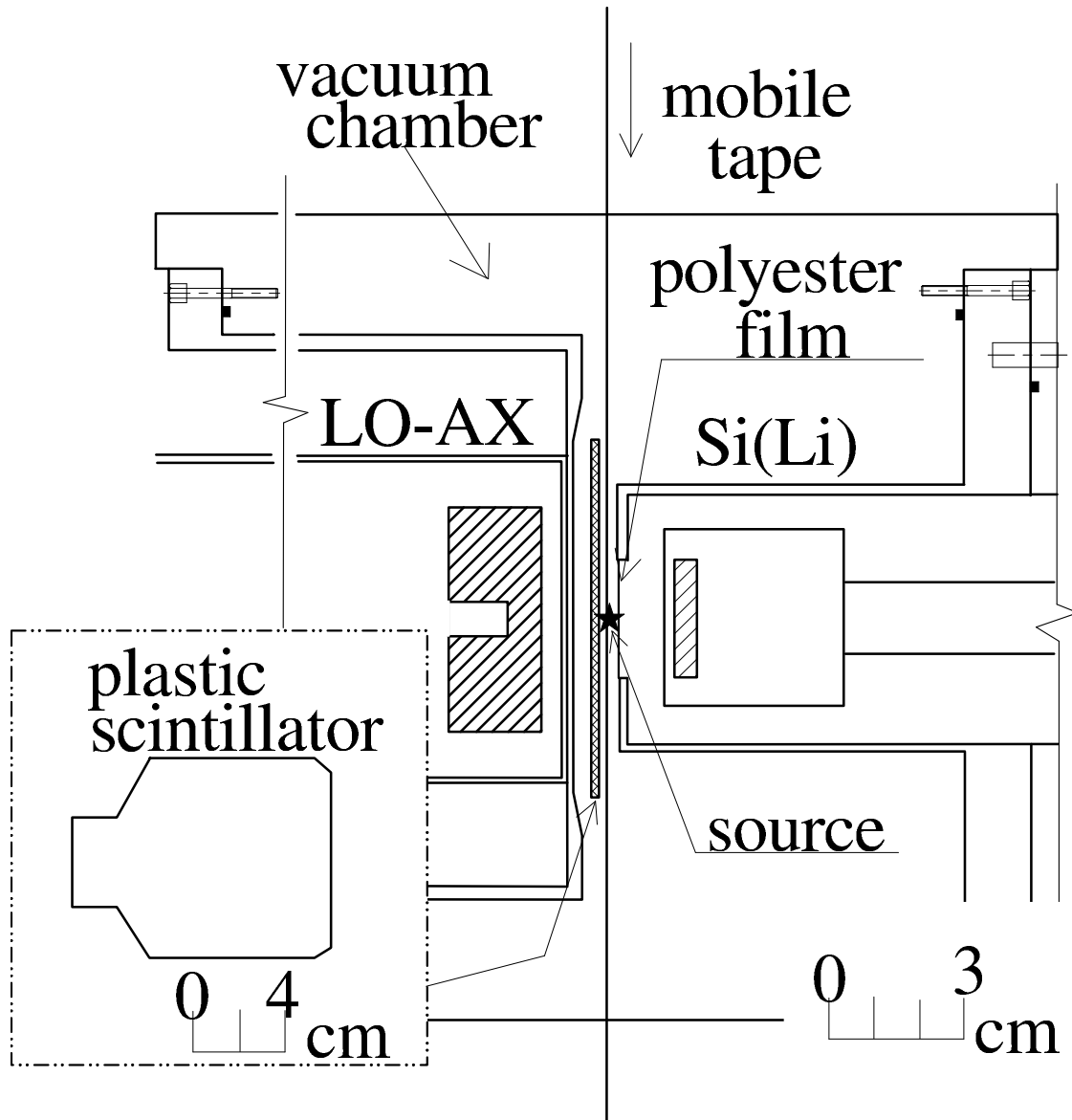


Fig. 1. A cross-sectional drawing of the detector setup for  $\beta$ - $\gamma$  and  $\beta$ -electron coincidence measurements.

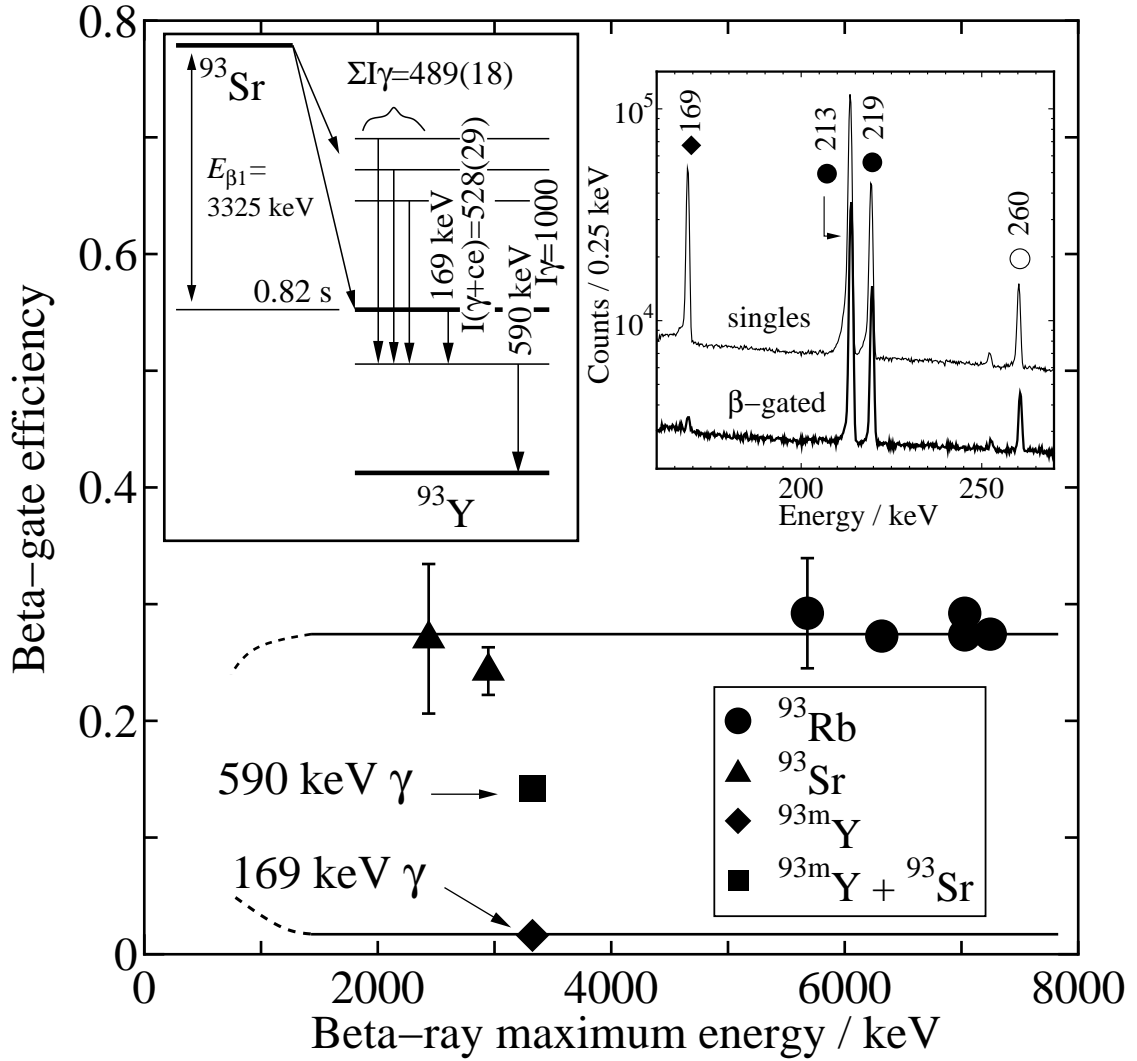


Fig. 2. Partial  $\gamma$  ray spectra observed in the singles and  $\beta$ -gated mode, and the  $\beta$ -gate efficiencies. The horizontal axis of the main figure means a  $\beta$ -ray maximum energy to a level populating a  $\gamma$  ray of interest; For example,  $E_{\beta 1}$  shown in a partial decay scheme of  $^{93}\text{Sr}$  and  $^{93\text{m}}\text{Y}$  [1] is the value for the 169-keV transition .

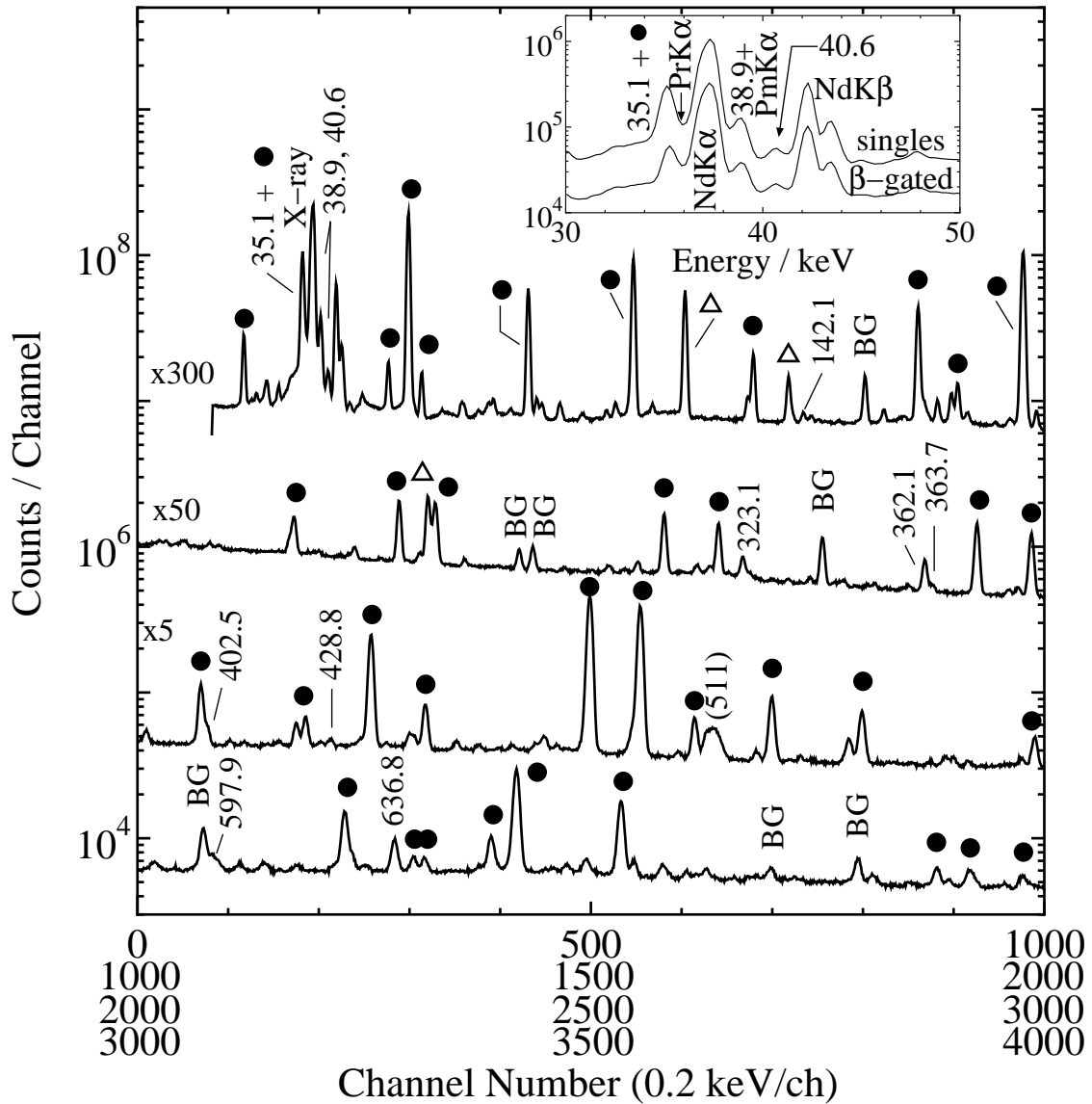


Fig. 3. Gamma-ray singles spectrum measured with a short-coaxial HPGe detector for a mass fraction 151+16. Gamma rays associated with the  $\beta^-$  decay of  $^{151}\text{Ce}$  are indicated with their energies in keV. Symbols of  $\bullet$  and  $\Delta$  mean  $\gamma$  rays from the decay of  $^{151}\text{Pr}$  and  $^{151}\text{Nd}$ , respectively. An inset shows a low-energy part of  $\gamma$  singles and a  $\beta$ -gated  $\gamma$  spectrum obtained in another experimental run.

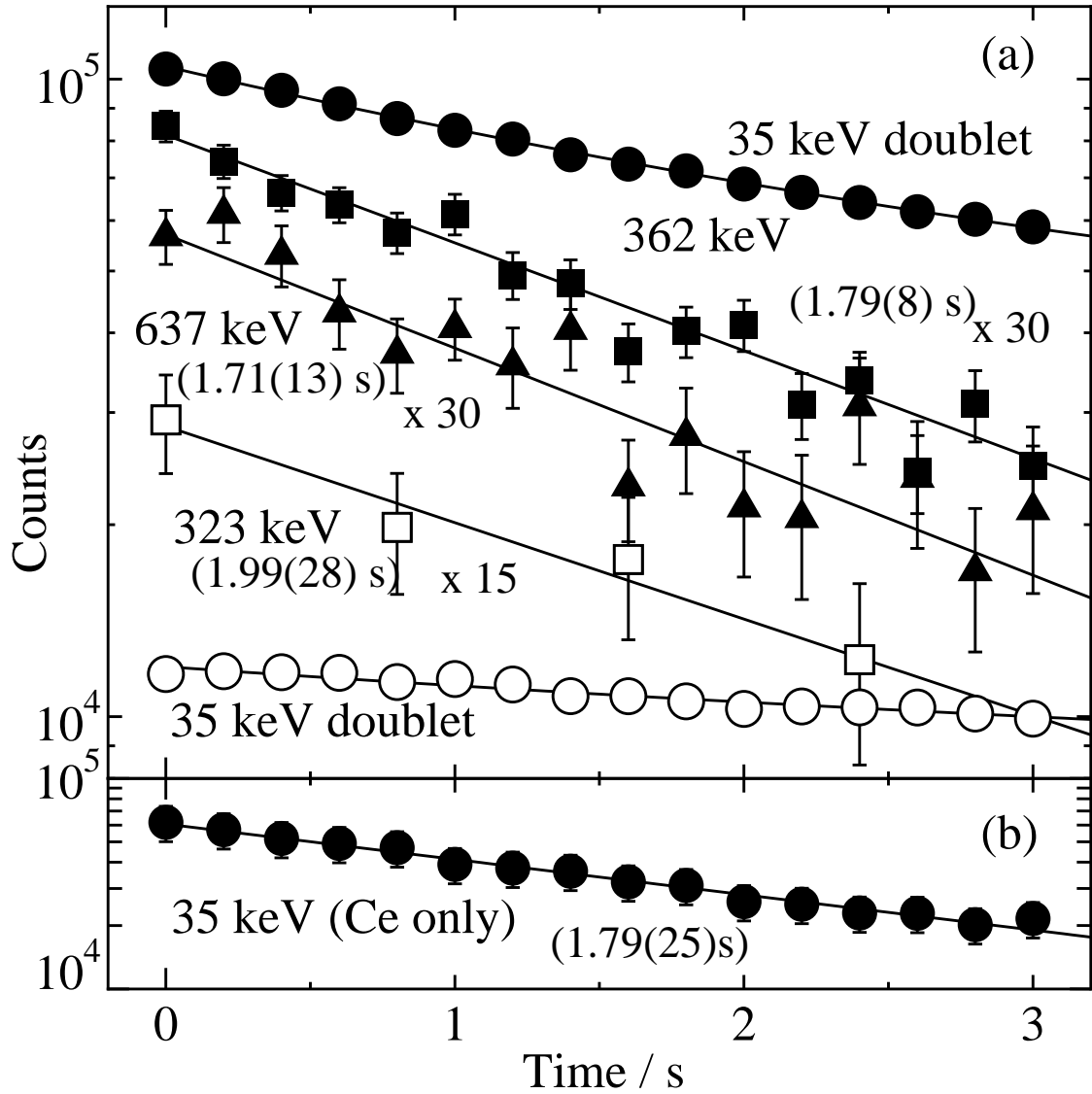


Fig. 4. (a) Decay curves of some  $\gamma$  rays from  $^{151}\text{Ce}$ . Closed and open marks mean data obtained from singles and  $\beta$ -gated measurements, respectively. Curves for the 35-keV  $\gamma$  doublet are fitted by a three-component function while the others by a single-component exponential one. (b) A decay curve containing only the 35-keV Ce  $\gamma$  ray (see text).

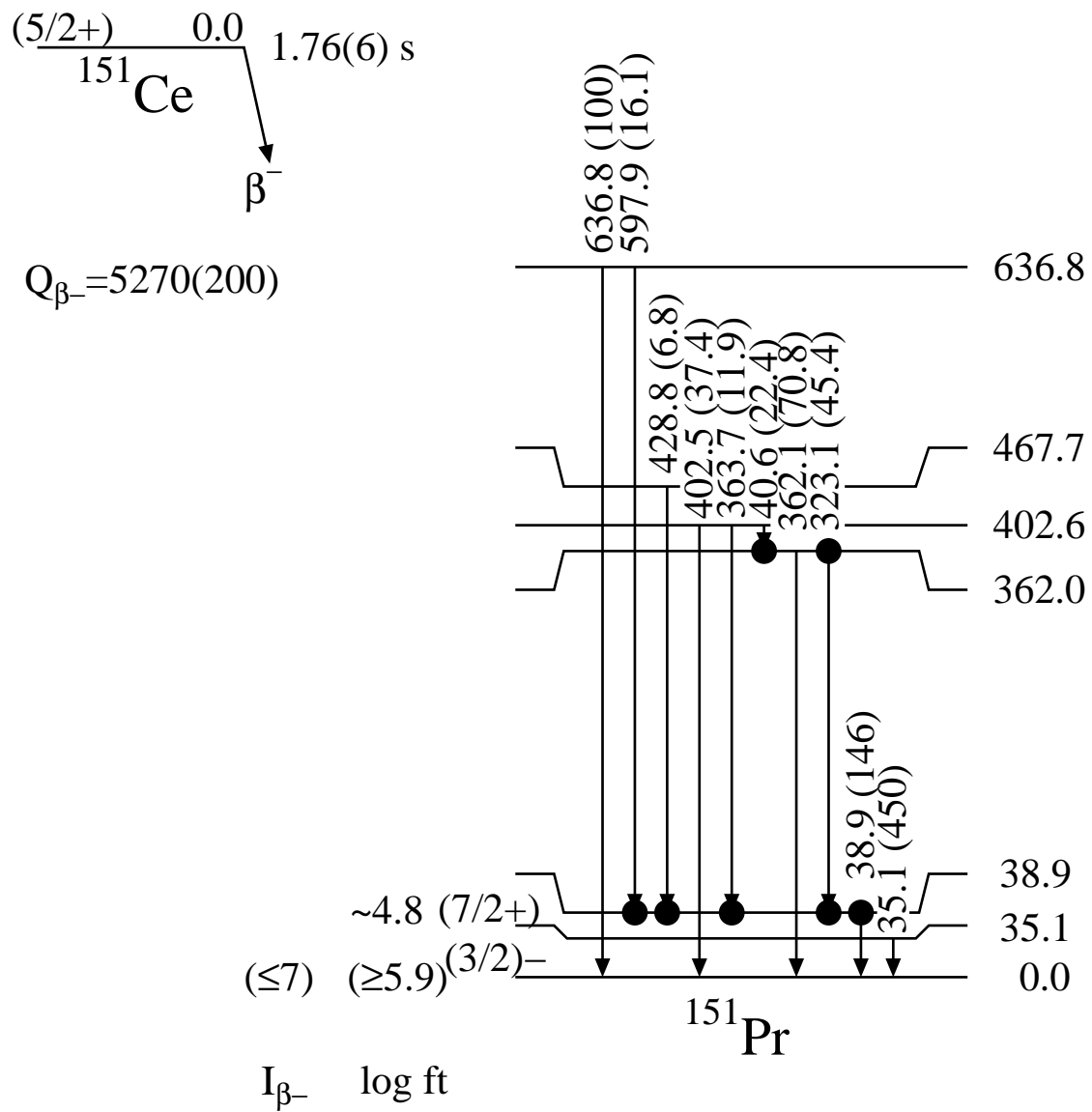


Fig. 5. A decay scheme of  $^{151}\text{Ce}$ . The  $Q_{\beta^-}$  value, spins and parities of the ground states are taken from previous studies [7,9,12].